Properties of the plant- and manure-derived biochars and their sorption of dibutyl phthalate and phenanthrene

Mengyi Qiu[1], Ke Sun[1], Jie Jin[1], Bo Gao[2], Yu Yan[1], Lanfang Han[1], Fengchang Wu[3] & Baoshan Xing[4]

[1]State Key Laboratory of Water Environment Simulation, School of Environment, Beijing Normal University, Beijing 100875, China, [2]State Key Laboratory of Simulation and Regulation of Water Cycle in River Basin, China Institute of Water Resources and Hydropower Research, Beijing 100038, China, [3]State Key Laboratory of Environmental Criteria and Risk Assessment, Chinese Research Academy of Environmental Sciences, Beijing 100012, China, [4]Stockbridge School of Agriculture, University of Massachusetts, Amherst, Massachusetts 01003, United States.

The properties of plant residue-derived biochars (PLABs) and animal waste-derived biochars (ANIBs) obtained at low and high heating treatment temperatures (300 and 450°C) as well as their sorption of dibutyl phthalate (DBP) and phenanthrene (PHE) were investigated in this study. The higher C content of PLABs could explain that CO_2-surface area (CO_2-SA) of PLABs was remarkably high relative to ANIBs. OC and aromatic C were two key factors influencing the CO_2-SA of the biochars. Much higher surface C content of the ANIBs than bulk C likely explained that the ANIBs exhibited higher sorption of DBP and PHE compared to the PLABs. H-bonding should govern the adsorption of DBP by most of the tested biochars and π-π interaction play an important role in the adsorption of PHE by biochars. High CO_2-SA (>200 m^2 g^{-1}) demonstrated that abundant nanopores of OC existed within the biochars obtained 450°C (HTBs), which likely result in high and nonlinear sorption of PHE by HTBs.

iochar is a byproduct from pyrolysis of carbon-rich biomass like grass, forestry products and animal manures[1]. The roles of biochars in biogeochemical cycles have received significant attention in recent years, since they could be used as soil amendments for helping biomass waste management[2], improving soil fertility and crop yield[3,4], and sequestrating carbon to mitigate climate change[5]. The properties and sorption strength of biochars have been reported to be affected by many factors, such as heating treatment temperatures (HTTs) and feedstock sources[6–9]. According to the HTTs, four distinct categories based on changes in the physical and chemical properties of the biochars could be identified: transition chars, amorphous chars, composite chars and turbostratic chars[10]. It has been reported that biochars obtained by pyrolyzing biomass at relative high temperature (HTT $\geq 500°C$) generally have simple structures, composed of large amounts of condensed aromatic C, and the sorption mechanisms are mainly adsorption-controlled. By contrast, biochars produced at relative low temperature (HTT $\leq 500°C$) are partially carbonized with high yields and complicated compositions, and contain diversified characteristics[1,6,11,12]. Previous study demonstrated that the sorption of hydrophobic organic compounds (HOCs) to biochars prepared at relatively low HTTs is composed of both adsorption on carbonized fractions and concurrent partition into the residual noncarbonized fractions[9]. Therefore, this study mainly focuses on the sorption of HOCs to low HTT biochars due to the complicacy in their sorption mechanisms stemmed from their complex chemical structures. Moreover, extensive studies reported that biochars could sorb lots of hazardous organic compounds, such as estrogens[13], pesticides[14], polychlorinated biphenyl (PCBs)[15], and polycyclic aromatic hydrocarbons (PAHs)[16,17]. However, the information about the sorption of phthalic acid esters (PAEs), as one kind of the emerging organic contaminants[18], by soils and sediments as well as biochars is still very limited[7,19,20]. In recent years, high production and wide application of PAEs in industry and agriculture created a big environmental problem. Humans use PAEs as plasticizers to induce workability and flexibility of polymeric materials. PAEs could enter soil, sediments, or even food through different pathways[21–23]. Unfortunately, this type of chemical has been suspected to have estrogenic effect as endocrine disruption compounds (EDCs) and has a potential tendency for bioaccumulation[24,25]. Some PAEs are suggested to be

Table 1 | Bulk elemental composition, ash content, atomic ratio, and CO_2-SA of biochars

biochars	C (%)	O (%)	H (%)	N (%)	Ash (%)	H/C	O/C	N/C	(O + N)/C	CO_2-SA[a]
CO300	67.1	20.7	4.6	1.3	6.3	0.83	0.23	0.02	0.25	243.6
PO300	59.1	19.7	5.2	4.0	12.1	1.05	0.25	0.06	0.31	103.4
LE300	62.2	16.9	5.4	4.8	10.7	1.04	0.20	0.07	0.27	90.3
RI300	55.3	19.5	3.7	0.8	20.6	0.81	0.26	0.01	0.28	188.5
WH300	63.3	24.0	4.4	0.5	7.8	0.84	0.28	0.01	0.29	162.3
MA300	63.8	25.3	5.1	0.8	5.1	0.95	0.30	0.01	0.31	188.3
NU300	60.9	29.2	5.4	0.2	4.3	1.06	0.36	0.00	0.36	40.5
WD300	65.4	27.3	5.3	0.0	2.0	0.97	0.31	0.00	0.31	155.0
CH300	10.0	4.6	0.9	0.6	83.9	1.10	0.34	0.05	0.40	31.4
SW300	36.5	14.9	3.6	3.2	41.8	1.18	0.31	0.08	0.38	89.6
CO450	71.6	13.3	3.9	1.2	10.1	0.65	0.14	0.01	0.15	367.1
PO450	61.9	14.3	3.7	3.7	16.4	0.72	0.17	0.05	0.22	222.0
LE450	63.4	12.6	3.7	5.0	15.2	0.70	0.15	0.07	0.22	248.6
RI450	57.9	11.8	3.3	0.8	26.2	0.69	0.15	0.01	0.16	293.4
WH450	70.2	12.9	4.3	0.5	12.2	0.73	0.14	0.01	0.14	349.7
MA450	74.4	11.8	3.8	1.0	9.1	0.61	0.12	0.01	0.13	388.3
NU450	78.4	11.8	3.6	0.3	6.0	0.54	0.11	0.00	0.12	394.1
WD450	75.9	16.7	3.7	0.1	3.7	0.58	0.16	0.00	0.17	601.6
CH450	9.8	3.6	0.9	0.5	85.2	1.12	0.28	0.05	0.33	33.2
SW450	33.7	10.2	2.6	2.6	50.9	0.91	0.23	0.07	0.29	162.0

[a]Calculated from nonlocal density functional theory (NLDFT) and grand canonical Monte Carlo simulation (GCMC) using CO_2 adsorption ($(m^2 g^{-1})$). CO, PO, LE, RI, WH, MA, NU, WD, CH and SW refer to the biochars produced from plant residues of cotton straw, potato straw, leaf, rice straw, wheat straw, maize straw, nut, wood dust (PLABs) and manures of chicken and swine (ANIBs). The numbers of 300 and 450 were represented to the heating treatment temperatures of the biochars (e.g., 300 and 450°C).

mutagens, hepatotoxic agents and carcinogens, which could cause toxic effects to human and wildlife[26]. Therefore, the environmental behavior of PAEs is becoming a hot area of research. Recently, Yang et al. reported that the soil carbon content has a crucial influence on sorption of PAEs by three soils[19]. If biochars are added to soil to improve fertility and store C: there is a potential for biochars and PAEs to interact. Therefore, our previous study about sorption of PAEs by grass- and wood-derived biochars has been carried out and proposed that amorphous biochars exhibit the greatest sorption capacity[7]. Also Sun et al. concluded that aliphatic and polar domains in biochars derived from only two plant-residues (e.g., low-mineral biochar) controlled the sorption of PAEs[7]. In order to confirm the conclusion, much more biochars derived from different feedstock sources (e.g., wood, grass, animal or poultry wastes) need to be further investigated. Additionally, it is worth noting that most sorption studies, to date, have used low-mineral biochars produced from relatively pure plant residues (e.g., plant residue-derived biochars (PLABs))[27], the sorption properties of HOCs to the high-mineral biochars (e.g., animal waste-derived biochars (ANIBs)) are rarely reported[28]. Although some of these contain considerable ash (e.g. grass biochar that contains substantial silica in the form of phytoliths)[7], the sorption properties of the ash component have not generally been considered. Especially, the recent studies demonstrated that the minerals within both biochars and soils have influence on the spatial arrangement or conformation of their organic matter (OM), in turn, which impacts on the sorption of phenanthrene (PHE) by the biochars or soils[28–31]. It is hypothesized that the minerals of biochars should play different role in the sorption between PAEs and PHE due to their different chemical properties, and also expected that the properties of ANIBs and PLABs should have different influence on sorption of PAEs. Some information about the sorption of PAEs and PHE by the six high-temperature biochars (HTBs) including ANIBs and PLABs produced at only high HTT (450°C) has been reported accompanying in our previous study[20], whose objective was to test the importance of the π-π electron donor−acceptor (EDA) interactions in the overall sorption of PHE and PAEs, respectively, onto the high-temperature biochars via competitive sorption of PHE, Dibutyl phthalate (DBP), and Cd^{2+} [20], however, the comprehensive sorption behavior of PAEs by both low-temperature biochars (LTBs) and HTBs and how the properties of these biochars would influence

the sorption of PAEs were poorly understand, which would be very important to precisely predict the fate of PAEs in the soils amended by the different kinds of biochars.

Therefore, the primary objectives of this study were to investigate how the properties of biochars influenced on the sorption of PAEs to a large number of LTBs and HTBs including the low-mineral PLABs and the high-mineral ANIBs, and further identify the different sorption mechanism between PAEs and PHE via analyzing the correlations of their sorption parameters to the bulk and surface structural characteristics of the biochars. We expect that this study could provide important information about agricultural and environmental application of biochars on immobilizing PAEs and PAHs. To meet these objectives, both ANIBs and PLABs were produced at low and high HTTs (300 and 450°C, respectively) to represent the high-mineral biochars and low-mineral biochars, respectively. The biochars produced at 300 and 450°C, respectively, were referred to LTBs and HTBs. DBP was chosen as a model of PAEs because the octanol-water partition coefficients of DBP and PHE are comparable. Furthermore, PHE, a typical representative of PAHs, was selected as a contrasting sorbate to explore dissimilar sorption mechanism between PAHs and PAEs to biochars due to their different molecular structure.

Results

Characterization of biochars. The bulk elemental composition, atomic ratio, ash content, and surface area determined by CO_2 (CO_2-SA) of 20 biochars produced at two different HTTs (300 and 450°C) are listed in Table 1. The C contents of PLABs were higher than ANIBs (Table 1), because the feedstocks of ANIBs had relatively more minerals than PLABs. However, their H/C ratios exhibited a reverse trend (Fig. 1a), suggesting that the higher degree of aromatization of organic matter (OM) associated with PLABs relative to OM within ANIBs. The relatively high H/C ratio of ANIB also indicated a great amount of original organic residues[9]. As H is primarily associated with OM, the H/C atomic ratios could be described as an indicator of carbonization[9]. In addition, ANIBs produced at 450°C had the remarkable high bulk (O + N)/C ratio (Fig. 1b), representing the presence of the polar functional groups in OM of the high HTTs ANIBs. The C contents increased with increasing HTT except for ANIBs (Table 1) and the values of
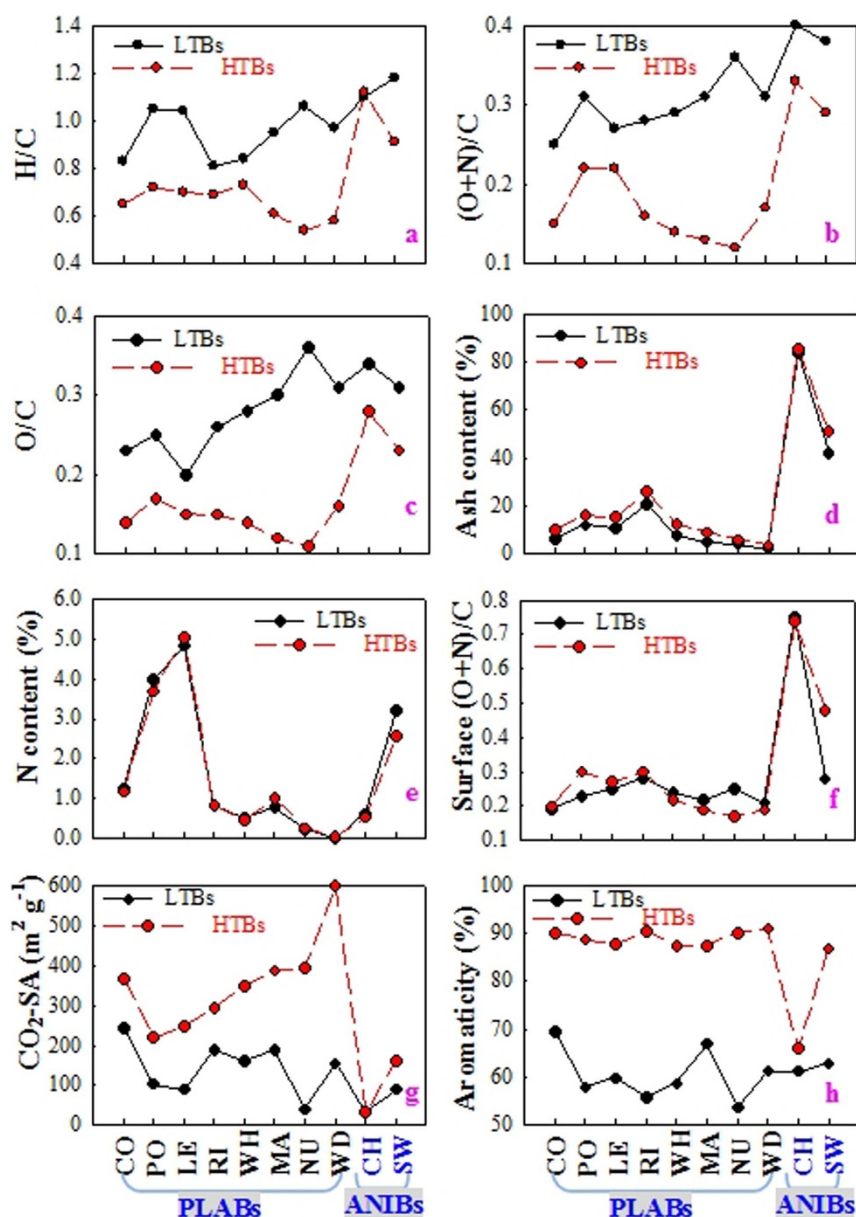
Figure 1 | Comparison of H/C atomic ratio (a), bulk polarity ((O + N)/C) (b), O/C atomic ratio (c), ash content (d), N content (e), surface polarity ((O + N)/C) (f), surface area determined by CO_2 adsorption (CO_2-SA) (g), and aromaticity (h) between the low-temperature biochars (LTBs) and high-temperature biochars (HTBs). CO, PO, LE, RI, WH, MA, NU, WD, CH and SW refer to the biochars produced from cotton straw, potato straw, leaf, rice straw, wheat straw, maize straw, nut, wood dust and manures of chicken and swine, respectively. Plant-residues and animal-waste derived biochars were named by PLABs and ANIBs, respectively. LTB and HTB represent the biochars obtained under pyrolysis or heat treatment temperature (HTT) at 300°C and 450°C, respectively.

polarity indexes (e.g., O/C and (O + N)/C) of LTBs were higher than those of HTBs (Fig. 1b and c), implying the enhancement of hydrophobicity[1] and reduction of polar functional groups with increasing HTT. However, no obvious reduction of O/C and (O + N)/C was observed for ANIBs compared to the remarkable reduction of O/C and (O + N)/C for PLABs (Fig. 1b and c), suggesting the minerals likely have a potential role in protecting the polar functional groups of OM within ANIBs from being removed during pyrolysis. The result was consistent with the previous studies that biochars produced at low HTTs were polar[1]. Both N and ash contents in the biochars were mostly constant with increasing HTT (Fig. 1d and e), indicating no distinct change of both N and ash during the charring process of these feedstocks.

The surface elemental composition and functional groups of the investigated biochars from X-ray photoelectron spectroscopy are presented in Table S1. The surface (O + N)/C values of ANIBs were obviously higher than PLABs (Table S1, Fig. 1f), which was consistent with the ash contents (Fig. 1d). Moreover, the ash content of the biochars were closely associated with the surface polarity ((O + N)/C) of the biochars ($R = 0.96$, $p < 0.01$, Fig. 2a). However, no significant positive correlation was observed between the ash contents and bulk polarity of the biochars (Fig. 2a). Therefore, it could be concluded that the minerals of the tested biochars could contribute to the high content of surface O of these biochars and their bulk O was mainly from the O of OM in these biochars.

Fourier transform infrared (FTIR) spectroscopy spectra of the 20 biochars as a function of feedstock sources and HTTs are shown in Fig. S1. References for the band assignments are provided in Table S2. The intense bands for aliphatic CH_2 disappear abruptly in the spectra of the HTBs and the disappearance of C=C ring stretching
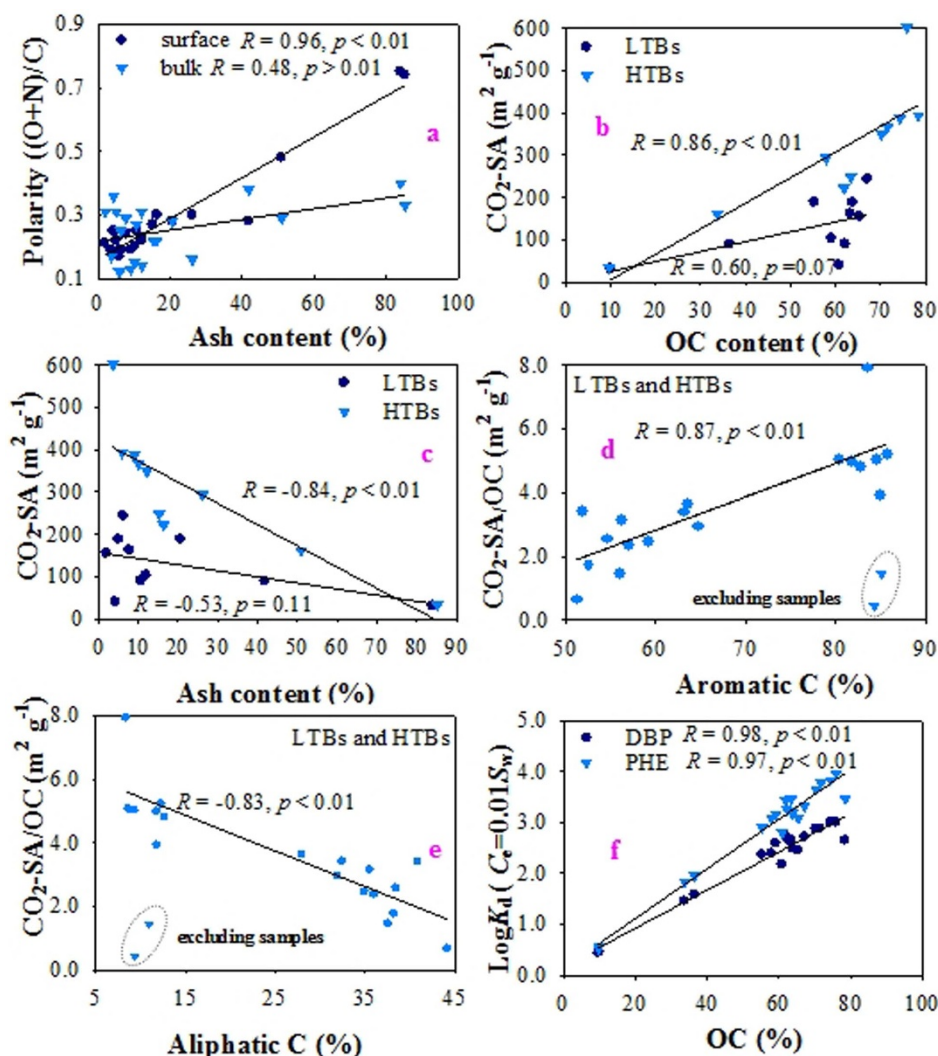
Figure 2 | Relationships between the bulk and surface polarity ((O + N)/C) of low-temperature biochars (LTBs) and high-temperature biochars (HTBs) and the ash content (a); between CO_2-surface area (CO_2-SA, determined using CO_2 adsorption) of LTBs and HTBs and their organic carbon (OC) content (b); between the CO_2-SA of the biochars and ash content (c); between the OC-normalized CO_2-SA (CO_2-SA/OC) and contents of aromatic C (d) and aliphatic C (e), respectively; and between $\log K_d$ ($C_e = 0.01 S_W$) of DBP and PHE and the OC contents of LTBs and HTBs (f).

vibration of lignin and plane bending of phenolic -OH related to syringyl units of lignin indicates the heat-induced decomposition of the feedstocks of PLABs. The polar functional groups (e.g.,-OH and C-O) are significantly reduced upon the HTTs. The band intensities for ester C=O, aromatic CO- and phenolic -OH groups of biochars diminished when the HTT reached to 450°C. Whereas C=C and C=O stretching vibrations in the aromatic rings were present when HTTs were elevated from 300 to 450°C. Three bands (885, 815, and 750 cm^{-1}) of out-of-plane deformations of aromatic -CH in the spectra increased with the elevated HTTs, indicating the formation of more condensed aromatic C. The ^{13}C-NMR spectra of the biochars and their integrated data of biochars are shown in Fig.S2 and Table S3, respectively. The quality of ANIBs ^{13}C-NMR spectra were affected by their high abundance of mineral and low C content (Fig. S2). The band intensity of aliphatic -CH$_2$-, carboxylic or carbonylic C and polar functional groups were significantly reduced with increasing HTT, which was consistent with the result of the FTIR spectra. The aromaticities of the investigated biochars were more than 55% (Table S3), indicating these biochars were mainly characterized with highly aromatic (aryl-dominated) structures.

CO_2-SA of PLABs (40.5–601.6 m^2 g^{-1}) was remarkably higher than those of ANIBs (31.4–162.0 m^2 g^{-1}) (Table 1). CO_2-SA of the biochars was elevated distinctly with increasing HTT (Fig. 1g). A significantly positive relationship between CO_2-SAs and organic carbon (OC) contents of ($R = 0.86$, $p < 0.01$, Fig. 2b) as well as a good negative correlation between CO_2-SAs and ash contents ($R = -0.84$, $p < 0.01$, Fig. 2c) was observed for the HTBs, suggesting that OC is a major contributor to CO_2-SAs of HTBs. Therefore, the higher C content of the PLABs compared to ANIBs could explain that the CO_2-SA of PLABs was much higher than ANIBs (Fig. 1g). As for the LTBs, besides the OC, the molecular composition of OC should be another factor in dominating the CO_2-SA. The CO_2-SA of biochars normalized by OC (CO_2-SA/OC) was correlated with the contents of the functional groups as indicated by the ^{13}C-NMR spectra of the biochars in order to find out other factors influencing the CO_2-SA of biochars. The CO_2-SA/OC of the biochars excluding the CO450 and PO450 was positively related to the aromatic C content (93–165 ppm) ($R = 0.87$, $p < 0.01$, Fig. 2d) and negatively related to the aliphatic C content (0–93 ppm) ($R = -0.83$, $p < 0.01$, Fig. 2e). Therefore, the increase of CO_2-SA of biochars with increasing HTT
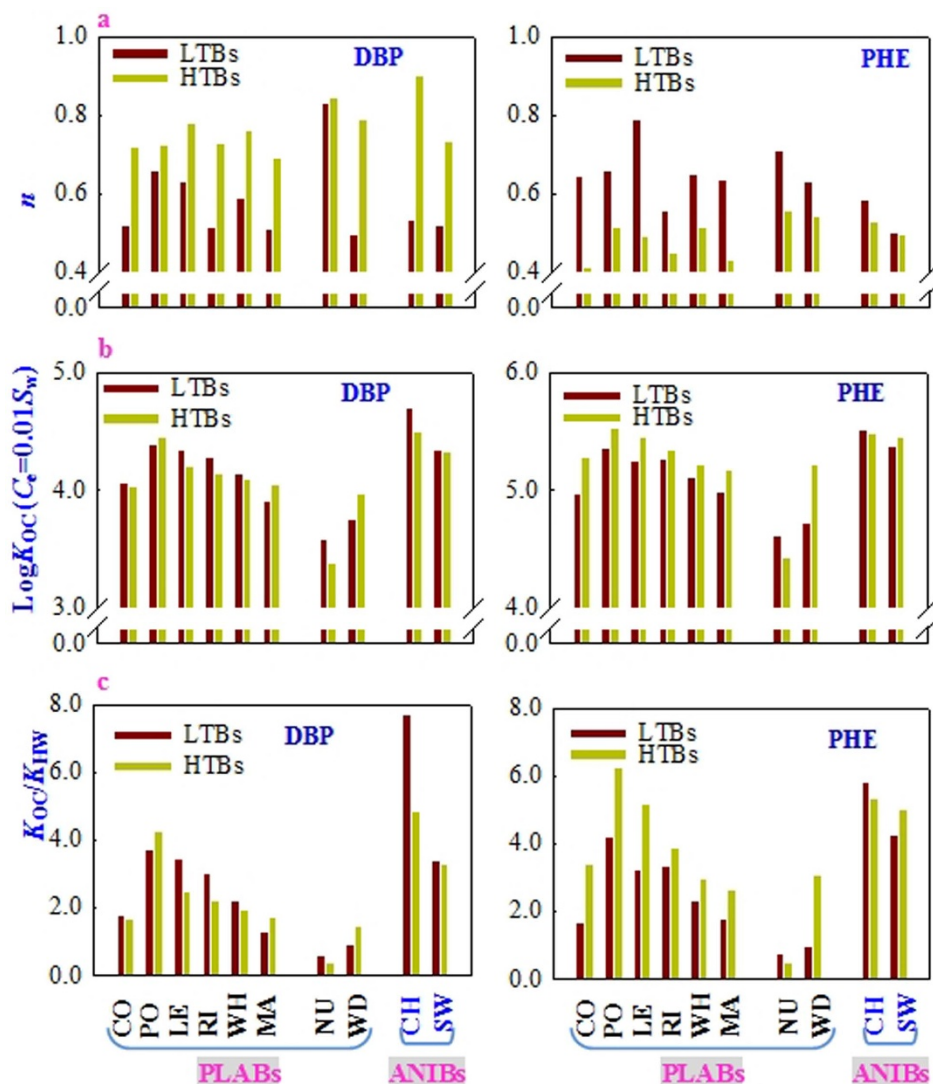
Figure 3 | Comparison of Freundlich nonlinearity coefficients (n) of DBP and PHE sorption isotherms (a), sorption capacity as indicated by the organic carbon (OC)-normalized distribution coefficient (logK_{OC}, mL g^{-1}) (b), and the K_{HW}-normalized K_{OC} values (K_{HW}, hexadecane-water partition coefficient) of DBP and PHE between the LTBs and HTBs (c). CO, PO, LE, RI, WH, MA, NU, WD, CH and SW refer to the biochars produced from cotton straw, potato straw, leaf, rice straw, wheat straw, maize straw, nut, wood dust and manures of chicken and swine, respectively. LTB and HTB represent the biochars obtained under pyrolysis or heat treatment temperature (HTT) at 300 and 450°C, respectively.

could be attributed to the elevated aromatic C of the biochars (Fig. 1g and h).

Adsorption of DBP and PHE by biochars. The sorption of PHE and DBP onto these 20 biochars is presented in Fig. S3, and was fitted well with Freundlich equation ($R^2 > 0.962$). The model parameters are listed in Table S4 and S5. The nonlinearity coefficients (n) derived from Freundlich model were significantly less than 1 ($p < 0.01$) (Fig. 3a). The low n values of biochars indicate heterogeneous glassy, rigid or condensed sorption domain and a wide site energy distribution in the biochars[32]. The majority of n values of DBP by the LTBs were lower than PHE by the LTBs, however, the opposite result was observed for the HTBs (Fig. 3a). Additionally, LTBs had lower isotherm nonlinearity (n) of DBP than HTBs, however, an inverse trend was observed for PHE (Fig. 3a). The significant and positive correlation of DBP sorption distribution coefficients (K_d) values of biochars to their OC contents was observed ($R = 0.97$, $p < 0.01$, Fig. 2f), suggesting that OC was one key factor in regulating the PAEs sorption by these biochars, consistent with the previous result that soil OC has been identified as a predominant sorbent for HOCs in soils and sediments as long as the total OC is >0.1%[33]. The OC

normalized concentration-specific sorption distribution coefficients (K_{OC}) values of biochars (Table S4 and S5) could be obtained from multiplying OC-normalized sorption capacity coefficient (K_F) by C_e^{n-1}. The logK_{OC} values of DBP or PHE varied with the different equilibrium concentrations due to their nonlinear sorption isotherm. ANIBs generally demonstrated the relatively high logK_{OC} values of DBP and PHE by both LTBs and HTBs (Fig. 3b). The higher surface C content of ANIBs than bulk C indicated that OM of ANIBs is likely distributed on the surface of their particles due to their abundant minerals, which thus let the solutes be easily accessible to the sorption domain of OM associated with the high-minerals ANIBs. As a result, this could likely account for that ANIBs exhibited relatively high sorption capacity (K_{OC}) of DBP and PHE compared to PLABs (Fig. 3b).

Discussion

In order to investigate how the properties of PLABs affect the sorption of DBP and PHE, the following discussion excluded the ANIBs to avoid the interference of the difference in the OM source between ANIBs and PLATs. The all correlation between the logK_{OC} values and
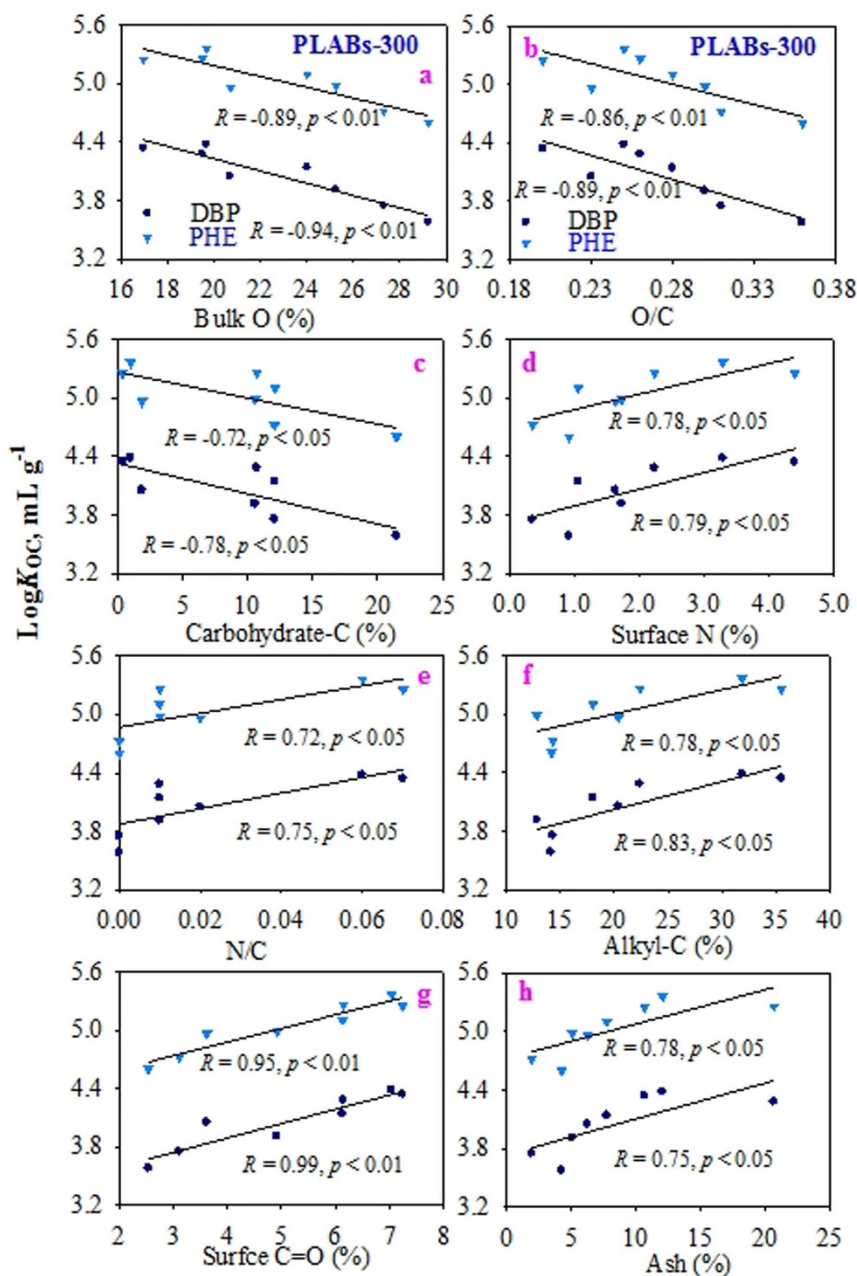
Figure 4 | Correlations between the organic carbon (OC)-normalized sorption distribution coefficient ($\log K_{OC}$, $C_e = 0.01S_W$ (the solubility of DBP or PHE in water at 20°C)) of DBP and PHE by the plant-derived biochars at 300°C (PLABs-300) and the content of bulk O (a) and bulk atomic ratio of O/C (b) as determined by the elemental analysis, carbohydrate-C (c) according to the ^{13}C-NMR results, the content of surface N (d) as indicated by XPS results, the bulk atomic ratio of N/C (e), the content of alkyl-C (f), the content of surface polar group of C=O (g), and the ash content (h) of PLABs-300.

properties of the PLABs produced at 300 and 450°C (PLABs-300 and PLABs-450), respectively, are presented in Fig. 4. For PLABs-300, the negative relationships between the $\log K_{oc}$ values and the contents of bulk O ($R \leq -0.89$, $p < 0.01$, Fig. 4a), the atomic ratio of O/C ($R \leq -0.86$, $p < 0.01$, Fig. 4b) and carbohydrate-C ($R \leq -0.78$ $p < 0.05$, Fig. 4c) were observed, implying that the O-containing polar groups of OM associated with the PLABs-300 may block the sorption of DBP and PHE. Moreover, DBP and PHE had the similar correlations between their $\log K_{OC}$ values and the parameters of the properties of the PLABs-300, demonstrating that DBP and PHE had the similar sorption mechanism during their sorption by the low-temperature PLABs containing the abundant O-containing polar groups. On the other hand, the $\log K_{OC}$ values of DBP and PHE were positively related to the content of the surface N ($R \geq 0.78$, $p < 0.05$,

Fig. 4d), the atomic ratio of bulk N/C ($R \geq 0.72$, $p < 0.05$, Fig. 4e), contents of alkyl-C according to the ^{13}C-NMR results ($R \geq 0.78$, $p < 0.05$, Fig. 4f) and the polar group of C=O as measured by the XPS results ($R \geq 0.95$, $p < 0.01$, Fig. 4g), and ash contents ($R \geq 0.75$, $p < 0.05$, Fig. 4h), suggesting that the minerals, alkyl-C, N-containing polar groups, and surface C=O associated with PLABs-300 could facilitate the sorption of both DBP and PHE, and that the H-bonding involving the N-containing polar groups of PLABs-300 should play the important role in the sorption. Additionally, for PLABs-450, the atomic ratios of O/C and H/C increased with the $\log K_{oc}$ values of DBP and PHE ($R \geq 0.77$, $p < 0.05$, Fig. 5a and b), indicating that the O-containing groups of OM within the PLABs-450 could benefit the sorption of DBP and PHE. The N-containing polar groups of low- and high-temperature PLABs played the same role in their DBP
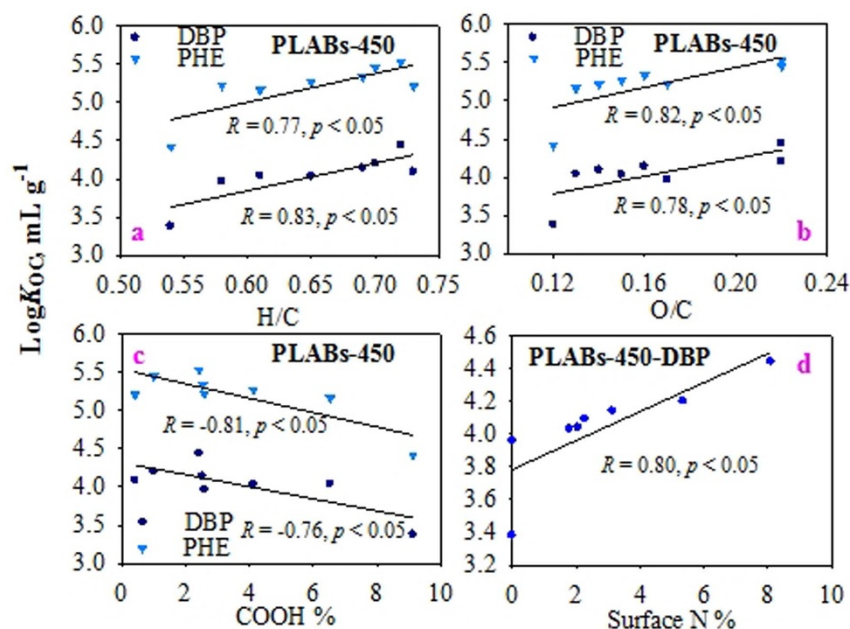
Figure 5 | Correlations between organic carbon (OC)-normalized sorption distribution coefficient ($\log K_{OC}$, $C_e = 0.01 S_W$ (the solubility of DBP or PHE in water at 20°C)) of DBP and PHE by plant-derived biochars at 450°C (PLABs-450) and the atomic ratios of H/C (a) and O/C (b), the percentages of COOH (c) determined by XPS results, and surface content of N (d).

sorption, however, N-containing polar groups of PLABs-450 had no positive impact on the sorption of PHE, suggesting DBP and PHE had different adsorption mechanisms. The sorption of both DBP and PHE by PLABs-300 decreased with their increasing bulk atomic ratio of O/C ($R \leq -0.86$, $p < 0.05$, Fig. 4b) while the corresponding sorption of DBP and PHE by PLABs-450 increased generally with the elevated the values of O/C ($R \geq 0.78$, $p < 0.05$, Fig. 5b), suggesting the most of O-containing polar groups of PLABs-300 likely blocked the sorption of both DBP and PHE because O functionality preferentially sorbs water molecules which could competitively block sorption of organic solutes proposed in other previous studies[34,35], however, these polar groups in PLABs-450 should play the positive role in the sorption of both DBP and PHE due to their involvement in the $\pi-\pi$ EDA interactions[36,37].

The $\log K_{oc}$ values of PHE of all biochars were obviously higher than those of DBP (Fig. 3b), which was similar to the order of their hydrophobicity as indicated by the hexadecane-water partition coefficient (K_{HW}) ($\log K_{HW} = 3.81$ for DBP[38] and $\log K_{HW} = 4.74$ for PHE[39]). As hexadecane is incapable of interactions such as π-π EDA interaction, polar interaction, and H-bonding, the K_{OC} values were normalized with hexadecane-water partition coefficient to exclude the hydrophobic effect[38] for investigating other sorption mechanisms apart from hydrophobic effect. After K_{HW} normalization, the K_{OC}/K_{HW} values of DBP and PHE by LTBs had no significant difference ($p = 0.446$, t-test) (Fig. 3c), while the significant difference in the K_{OC}/K_{HW} values between DBP and PHE were observed for HTBs ($p = 0.000$, t-test) and for HTBs K_{OC}/K_{HW} values of PHE were generally higher than DBP (Fig. 3c), suggesting that DBP and PHE have the same chance to be involved in the adsorption by LTBs, however, PHE should be more readily to reach the adsorption sites of the HTBs compared to DBP due to PHE being a planar molecule.

The Os of the ester groups on DBP are able to act as H-bonding acceptors. It could form H-bonds through the water molecules[40]. It has been reported that H of the hydroxyl group (H-bonding donors) on biochars can directly form the H-bonds with the DBP molecule[33]. So DBP (hydrogen bond-forming ability: HB = 8.0[41]) could be strongly sorbed on biochars through bridging water molecules or on H-donating functional groups. Additionally, it was reported that

apolar PHE as an aromatic hydrocarbon might have some ability to act as a weak H-acceptor[39,42,43] with low energies as a result of its weak H-bonding ability (HB = 0.2[44]). Therefore, H-bonding of DBP/PHE may act in addition to hydrophobic interaction. The significant positive correlations between $\log K_{OC}$ ($C_e = 0.01 S_w$) values of both DBP and PHE and surface N of PLABs ($R \geq 0.78$, $p < 0.05$, Fig. 4d and $R = 0.80$, $p < 0.05$, Fig. 5d) along with the higher K_{OC} of ANIBs (containing high polarity) than PLABs were observed (Fig. 3b), both supporting that the above conclusion that the H-bonding interaction should partly play the role in the overall sorption of DBP and PHE by these tested biochars. If H-bonding interaction regulated the overall sorption of DBP and PHE on biochars, the n values of their isotherms by the biochars should be negatively correlated with the polarity. Coincidentally, this negative correlation was only observed for the DBP sorption by the tested biochars excluding NU300 and CH450 ($R \leq -0.77$ $p < 0.05$, Fig. 6a), however, the reverse relationship between the isotherm n values of PHE by the biochars excluding LE300 and the polarity was detected ($R \geq 0.58$, $p \leq 0.01$, Fig. 6a), suggesting that H-bonding interaction could affect the overall adsorption of DBP by most of the tested biochars, but not the major specific interactions between PHE and these biochars. It was also noted that the significant and negative correlation between n of PHE and aromaticity of the biochars was obtained ($R = -0.75$, $p < 0.01$, Fig. 6b) combined with the significant and positive relationship between $\log K_{OC}$ values of PHE and the surface polarity of PLABs-450 ($R \geq 0.78$, $p < 0.05$, Fig. 5b), which was attributed to the enhanced π acceptor ability of biochars with increasing electron-withdrawing polar moieties on biochar surface[7], suggesting that the major specific interactions between PHE (π-donor) and biochars should be the π-π interaction because recent studies suggest that PHE could sever as a π-donor to interact with the π-acceptor moieties in soil humic substances[45]. Additionally, enhancement of the $\log K_{OC}$ values (Fig. 3b) and reduction of n values for PHE from LTBs to HTBs (Fig. 3a) as a result of the increasing of aromaticity (Fig. 1h) and decreasing N- or O-containing polar groups (Fig. 1b and c), and the opposite trend in the change of both $\log K_{OC}$ values and DBP isotherm n values (Fig. 3) also both support that the π-π interaction should mainly contribute to the specific interactions between PHE
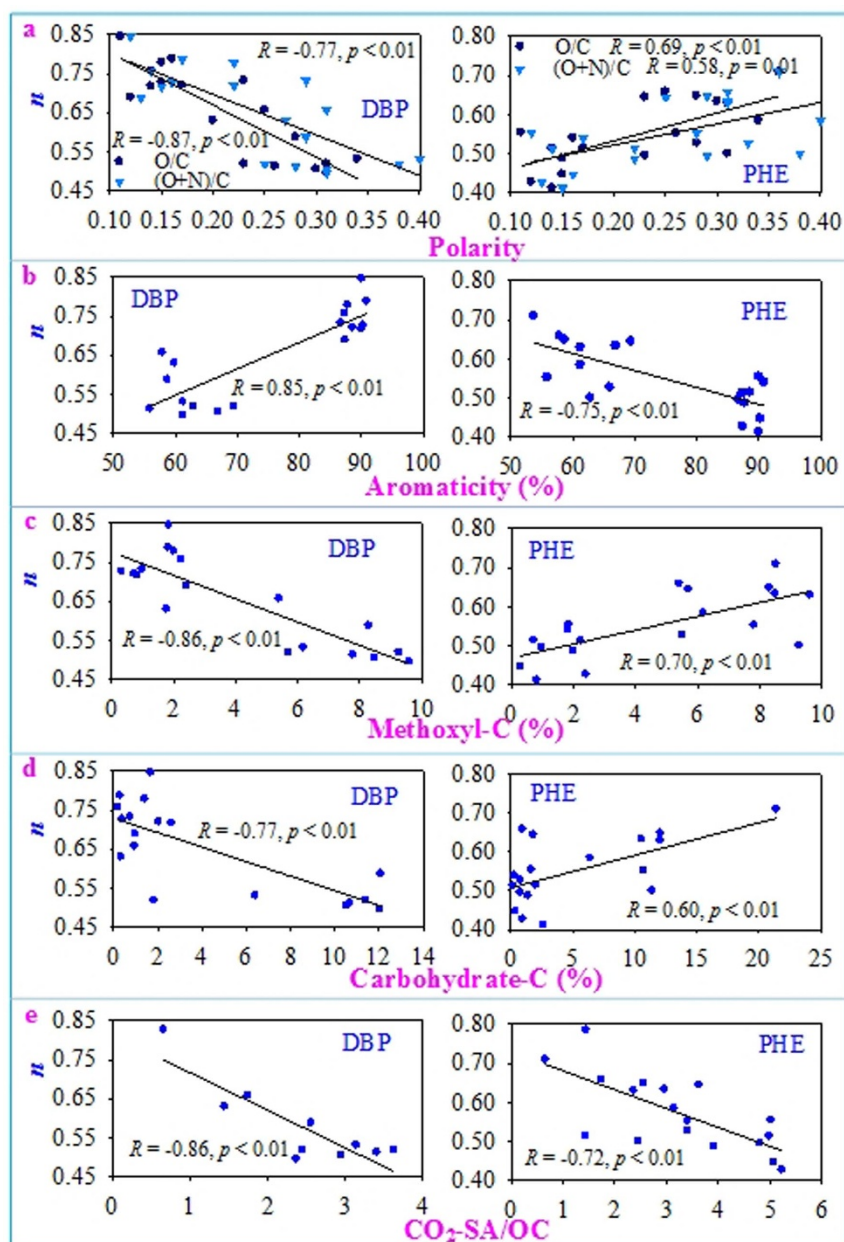
Figure 6 | Correlations between the Freundlich nonlinearity coefficients (n) of DBP and PHE sorption isotherms of DBP and PHE by the biochars and the polarity (($N + O$)/C and O/C) (a), and contents of the aromaticity (b), methoxyl-C (c), and carbohydrate-C (d) obtained by ^{13}C-NMR, and organic carbon (OC)-normalized surface area as determined by CO_2 adsorption (CO_2-SA/OC) (e) of the biochars.

and biochars while the H-bonding likely regulate the adsorption of DBP by the biochars.

Besides the specific adsorption mechanism, pore-filling was concluded to be the most important sorption mechanism for PAHs with flat aromatic sorbent surfaces[46]. Aromatic C increased with increasing HTT, leading to the elevated SAs of biochars (Fig. 2d). Moreover, from LTBs to HTBs, the increased CO_2-SA values were consistent with the enhancement of the logK_{OC} values and reduction of n values for PHE (Fig. 3a and b). Hence, it could be concluded that pore-filling mechanism may play an important role in PHE adsorption by most of the tested biochars. Especially for HTBs, the remarkably high CO_2-SA (>200 m^2 g^{-1}, Table 1) demonstrated that more nanopores existed within the biochars (Fig. S4), which could be responsible for the strong nonlinearity of sorbates, further supporting that PHE sorption by HTBs had generally stronger nonlinear and higher sorption capacity than LTBs (Fig. 3b).

Methods

Chemicals. DBP (99+%) and PHE (98+%) were purchased from Dr. Ehrenstorfer GmbH (Augsburg, Germany) and Sigma-Aldrich Chemical Co, respectively. DBP and PHE were individually dissolved in methanol as stock solution, and stored at 4°C in the dark. The water solubilities (S_w) of DBP and PHE are 11.2 mg L^{-1} and 1.12 mg L^{-1}, respectively[47,48].

Biochars preparation. A total of 20 biochars were used in this study. Detailed information about the biochars preparation was reported elsewhere[28]. Briefly, two kinds of feedstock materials, including straws of cotton, potato, rice, wheat and maize, leaves, nutshells, wood dust and animal manure wastes of chicken and swine, were selected to obtain the PLABs and ANIBs, respectively. Here, biochars were referenced according to feedstock source materials (plant residues: cotton straw, potato straw, leaf, rice straw, wheat straw, maize straw, nut and wood dust; animal-waste: manures of chicken and swine) (i.e., CO, PO, LE, RI, WH, MA, NU, WD, CH and SW) and HTTs (300 and 450°C) (i.e., CO300, CO450, PO300, PO450, LE300, LE450, RI300, RI450, WH300, WH450, MA300, MA450, NU300, NU450, WD300, WD450, CH300, CH450, SW300 and SW450). PLABs could be classified as grass-like biochars (GBs) including the biochars produced from CO, PO, LE, RI, WH, and MA and

wood-like biochars (WBs) including the biochars obtained from the NU and WD. The biochars produced at low and high temperature (300 and 450°C, respectively) were named as LTBs and HTBs, respectively.

Characterization of biochars. The bulk C, H, N and O contents of the biochars were determined using an Elementar Vario ELIII elemental analyzer (Elementar Company, Germany). Ash content was determined by heating biochars at 750°C for 4 h. The microporosity and cumulative surface area (CO$_2$-SA) of biochars were obtained by Autosorb-1 gas analyzer (Quantachrome Instrument Corp., Boynton Beach, FL) using CO$_2$ isotherm at 273 K[49]. Surface elemental composition (e.g., C, O, N, and Si) as well as the carbon-based functional group distribution of biochars were examined by using X-ray photoelectron spectroscopy (XPS) with a Kratos Axis Ultra electron spectrometer using monochromated Al Kα source operated at 225 W, including an elemental survey scan and a high-resolution scan at the C$_{1s}$ edge[50]. Fourier transform infrared (FTIR) spectroscopy spectra were recorded by a Nexus 670 FTIR spectrophotometer (Thermo Nicolet Corporation, US). The ^{13}C nuclear magnetic resonance (^{13}C-NMR) spectra of biochars were obtained by using CPMAS (solid-state cross-polarization magic angle spinning) technique. More detailed information about the characterization procedures of FTIR, ^{13}C-NMR, and XPS as well as the chemical shift assignments of ^{13}C-NMR was described in detail elsewhere[14].

Sorption experiments of DBP and PHE by biochars. A batch equilibration technique was used to obtain the sorption isotherms of DBP and PHE to 20 biochars. The stock solution was diluted sequentially in background solution which containing 200 mg L^{-1} NaN$_3$ (as bio-inhibitor) and 0.01 M CaCl$_2$ (as ionic strength adjuster) to 10 different concentrations (100–10,0000 μg L^{-1} for DBP, and 2–1100 μg L^{-1} for PHE). The sorption experiments were conducted using 15 ml and 40 ml glass vials with Teflon-lined screw caps. After shaking at 100 rpm for about 1 h, the test solution of DBP or PHE was added to vials with appropriate amount of biochars until the head space was kept minimal to avoid any potential vapor loss. The amount of biochars was selected to obtain 20–80% uptake of initially added DBP or PHE at equilibrium. All vials were sealed and continuously shaken at room temperature (23°C) for 7 d (DBP) and 10 d (PHE), respectively, according to the preliminary test. All experiments including the blanks were conducted in duplicates. In addition, blank experiments showed that the loss of DBP and PHE in both systems were insignificant. Hence, uptakes of DBP and PHE by biochars were calculated by mass balance.

Detection of solutes. After being shaken on the rotary shaker for 7 d or 10 d at room temperature, the vials were centrifuged at 3000 rpm for 30 min, then 2 mL supernatant was transferred from each sample and added to the 2 mL vial for analyzing the sorbate concentration in solution phase by HPLC (1260 Series, Agilent Technolohies, Santa Clara, CA) equipped with reversed-phase C18 analytical column (5 μm, 250 mm × 4.6 mm). DBP was detected by a UV detector with the detection wavelength set at 228 nm. The mobile phase consisted of 80% acetonitrile and 20% ultrapure water at a flow rate of 1 mL min^{-1}. Low concentration of PHE was analyzed with a fluorescence detector with excitation wavelength set at 250 nm and emission wavelength set at 364 nm. UV detector at 250 nm was applied to determine the concentrations which were higher than 50 μg L^{-151}. The mobile phase consisted of 90% methanol and 10% ultrapure water at a flow rate of 0.8 mL min^{-1}. The injection volume was 20 μL, and temperature of the column was 35°C.

Statistical analysis. The detected and calculated biochars-sorbed DBP/PHE (q_e) and freely-dissolved DBP/PHE (C_e) concentrations could form sorption curves and the sorption curves were fitted with Freundlich model (logarithmic form):

$$\log q_e = \log K_F + n \log C_e \tag{1}$$

where q_e (μg g^{-1}) is the solid-phase concentration and C_e (μg L^{-1}) represents liquid-phase free concentration. K_F ((μg g^{-1})/(μg L^{-1})^n) is the sorption affinity-related coefficient, and n is the nonlinearity factor. The quality of the fitting was determined using SigmaPlot 10.0 and statistical analysis (Pearson correlation analysis and t-test) was performed using SPSS 18.0.

1. Novak, J. M. et al. Characterization of designer biochar produced at different temperatures and their effects on a loamy sand. *Ann. Environ. Sci.* **3**, 195–206 (2009).
2. Roberts, K. G., Gloy, B. A., Joseph, S., Scott, N. R. & Lehmann, J. Life cycle assessment of biochar systems: estimating the energetic, economic, and climate change potential. *Environ. Sci. Technol.* **44**, 827–833 (2009).
3. Chan, K. G., Van Zwieten, L., Meszaros, I., Downie, A. & Joseph, S. Using poultry litter biochars as soil amendments. *Soil Res.* **46**, 437–444 (2008).
4. Sohi, S. P., Krull, E., Lopez-Capel, E. & Bol, R. A review of biochar and its use and function in soil. *Adv. Agron.* **105**, 47–82 (2010).
5. Lehmann, J., Gaunt, J. & Rondon, M. Bio-char sequestration in terrestrial ecosystems–a review. *Mitig. Adapt. Strat. Gl.* **11**, 395–419 (2006).
6. Chen, B., Zhou, D. & Zhu, L. Transitional adsorption and partition of nonpolar and polar aromatic contaminants by biochars of pine needles with different pyrolytic temperatures. *Environ. Sci. Technol.* **42**, 5137–5143 (2008).
7. Sun, K. et al. Polar and aliphatic domains regulate sorption of phthalic acid esters (PAEs) to biochars. *Bioresource Technol.* **118**, 120–127 (2012).
8. Uchimiya, M., Wartelle, L. H., Klasson, K. T., Fortier, C. A. & Lima, I. M. Influence of pyrolysis temperature on biochar property and function as a heavy metal sorbent in soil. *J. Agr. Food chem.* **59**, 2501–2510 (2011).
9. Chun, Y., Sheng, G., Chiou, C. T. & Xing, B. Compositions and sorptive properties of crop residue-derived chars. *Environ. Sci. Technol.* **38**, 4649–4655 (2004).
10. Harvey, O. R., Herbert, B. E., Rhue, R. D. & Kuo, L.-J. Metal interactions at the biochar-water interface: energetics and structure-sorption relationships elucidated by flow adsorption microcalorimetry. *Environ. Sci. Technol.* **45**, 5550–5556 (2011).
11. Glaser, B., Lehmann, J. & Zech, W. Ameliorating physical and chemical properties of highly weathered soils in the tropics with charcoal–a review. *Biol. Fert. Soils* **35**, 219–230 (2002).
12. Keiluweit, M., Nico, P. S., Johnson, M. G. & Kleber, M. Dynamic molecular structure of plant biomass-derived black carbon (biochar). *Environ. Sci. Technol.* **44**, 1247–1253 (2010).
13. Sun, K. et al. Sorption of bisphenol A, 17α-ethinyl estradiol and phenanthrene on thermally and hydrothermally produced biochars. *Bioresource Technol.* **102**, 5757–5763 (2011).
14. Zhang, G. et al. Sorption of simazine to corn straw biochars prepared at different pyrolytic temperatures. *Environ. Pollut.* **159**, 2594–2601 (2011).
15. Pignatello, J. J., Kwon, S. & Lu, Y. Effect of natural organic substances on the surface and adsorptive properties of environmental black carbon (char): attenuation of surface activity by humic and fulvic acids. *Environ. Sci. Technol.* **40**, 7757–7763 (2006).
16. Chen, G. et al. Effects of copper, lead, and cadmium on the sorption and desorption of atrazine onto and from carbon nanotubes. *Environ. Sci. Technol.* **42**, 8297–8302 (2008).
17. Wang, X. & Xing, B. Sorption of organic contaminants by biopolymer-derived chars. *Environ. Sci. Technol.* **41**, 8342–8348 (2007).
18. Clarke, B. O. & Smith, S. R. Review of 'emerging' organic contaminants in biosolids and assessment of international research priorities for the agricultural use of biosolids. *Environ.Int.* **37**, 226–247 (2011).
19. Yang, F., Wang, M. & Wang, Z. Sorption behavior of 17 phthalic acid esters on three soils: effects of pH and dissolved organic matter, sorption coefficient measurement and QSPR study. *Chemosphere* **93**, 82–89 (2013).
20. Jin, J. et al. Single-solute and bi-solute sorption of phenanthrene and dibutyl phthalate by plant- and manure-derived biochars. *Sci. Total Environ.* **473–474**, 308–316 (2014).
21. Fromme, H. et al. Occurrence of phthalates and bisphenol A and F in the environment. *Water Res.* **36**, 1429–1438 (2002).
22. He, H. et al. Trace analysis of persistent toxic substances in the main stream of Jiangsu section of the Yangtze River, China. *Environ.Sci. Pollut. R.* **18**, 638–648 (2011).
23. Zeng, F. et al. Distribution of phthalate esters in urban soils of subtropical city, Guangzhou, China. *J. Hazard. Mater.* **164**, 1171–1178 (2009).
24. Harris, C. A., Henttu, P., Parker, M. G. & Sumpter, J. P. The estrogenic activity of phthalate esters in vitro. *Environ. Health Persp.* **105**, 802–811 (1997).
25. Zacharewski, T. R. et al. Examination of the in vitro and in vitroestrogenic activities of eight commercial phthalate esters. *Toxicol. Sci.* **46**, 282–293 (1998).
26. Huff, J. E. & Kluwe, W. M. Phthalate esters carcinogenicity in F344/N rats and B6C3F1 mice. *Prog. Clin. Biol. Res.* **141**, 137–54 (1984).
27. Smernik, R. J. Biochar and sorption of organic compounds. *Biochar for Environmental Management: Science and Technology* (Eds Lehmann, J. & Joseph, S. Earthscan, Ltd.: London, 2009) 289–300 (2009).
28. Sun, K. et al. Impact of deashing treatment on biochar structural properties and potential sorption mechanisms of phenanthrene. *Environ. Sci. Technol.* **47**, 11473–11481 (2013).
29. Feng, X., Simpson, A. J. & Simpson, M. J. Investigating the role of mineral-bound humic acid in phenanthrene Sorption. *Environ. Sci. Technol.* **40**, 3260–3266 (2006).
30. Sun, K. et al. Isolation and characterization of different organic matter fractions from a same soil source and their phenanthrene sorption. *Environ. Sci. Technol.* **47**, 5138–5145 (2013).
31. Yang, Y., Shu, L., Wang, X., Xing, B. & Tao, S. Impact of de-ashing humic acid and humin on organic matter structural properties and sorption mechanisms of phenanthrene. *Environ. Sci. Technol.* **45**, 3996–4002 (2011).
32. Pignatello, J. J. & Xing, B. Mechanisms of slow sorption of organic chemicals to natural particles. *Environ. Sci. Technol.* **30**, 1–11 (1995).
33. Schwarzenbach, R. P. & Westall, J. Transport of nonpolar organic compounds from surface water to groundwater. Laboratory sorption studies. *Environ. Sci. Technol.* **15**, 1360–1367 (1981).
34. Snoeyink, V. L. & Weber, W. J. The surface chemistry of active carbon; a discussion of structure and surface functional groups. *Environ. Sci. Technol.* **1**, 228–234 (1967).
35. Kaneko, Y., Abe, M. & Ogino, K. Adsorption characteristics of organic compounds dissolved in water on surface-improved activated carbon fibres. *Colloids Surf.* **37**, 211–222 (1989).
36. Zhu, D. & Pignatello, J. J. Characterization of aromatic compound sorptive interactions with black carbon (charcoal) assisted by graphite as a model. *Environ. Sci. Technol.* **39**, 2033–2041 (2005).

37. Sander, M. & Pignatello, J. J. Characterization of charcoal adsorption sites for aromatic compounds: insights drawn from single-solute and bi-solute competitive experiments. *Environ. Sci. Technol.* **39**, 1606–1615 (2005).

38. Wang, F., Yao, J., Sun, K. & Xing, B. Adsorption of dialkyl phthalate esters on carbon nanotubes. *Environ. Sci. Technol.* **44**, 6985–6991 (2010).

39. Abraham, M. H., Chadha, H. S., Whiting, G. S. & Mitchell, R. C. Hydrogen bonding. 32. An analysis of water-octanol and water-alkane partitioning and the Δlog p parameter of seiler. *J. Pharm. Sci.* **83**, 1085–1100 (1994).

40. Zhang, W. *et al.* Equilibrium and heat of adsorption of diethyl phthalate on heterogeneous adsorbents. *J. Colloid Interf. Sci.* **325**, 41–47 (2008).

41. Tantishaiyakul, V., Worakul, N. & Wongpoowarak, W. Prediction of solubility parameters using partial least square regression. *Int. J. Pharmaceut.* **325**, 8–14 (2006).

42. Abraham, M. H., Andonian-Haftvan, J., Whiting, G. S., Leo, A. & Taft, R. S. Hydrogen bonding. Part 34. The factors that influence the solubility of gases and vapours in water at 298 K, and a new method for its determination. *J. Chem. Soc., Perkin Trans.* **2**, 1777–1791 (1994).

43. Zhu, D., Hyun, S., Pignatello, J. J. & Lee, L. S. Evidence for π-π electron donor-acceptor interactions between π-donor aromatic compounds and π-acceptor sites in soil organic matter through pH effects on sorption. *Environ. Sci. Technol.* **38**, 4361–4368 (2004).

44. Kamlet, M. J., Doherty, R. M., Abraham, M. H., Marcus, Y. & Taft, R. W. Linear solvation energy relationship. 46. An improved equation for correlation and prediction of octanol/water partition coefficients of organic nonelectrolytes (including strong hydrogen bond donor solutes). *J. Phys. Chem.* **92**, 5244–5255 (1988).

45. Wijnja, H., Pignatello, J. J. & Malekani, K. Formation of π–π complexes between phenanthrene and model π-acceptor humic subunits. *J. Environ. Qual.* **33**, 265–275 (2004).

46. Jonker, M. T. O. & Koelmans, A. A. Sorption of polycyclic aromatic hydrocarbons and polychlorinated biphenyls to soot and soot-like materials in the aqueous environment: mechanistic considerations. *Environ. Sci. Technol.* **36**, 3725–3734 (2002).

47. Sullivan, K. F., Atlas, E. L. & Giam, C. S. Adsorption of phthalic acid esters from seawater. *Environ. Sci. Technol.* **16**, 428–432 (1982).

48. Grimberg, S. J., Nagel, J. & Aitken, M. D. Kinetics of phenanthrene dissolution into water in the presence of nonionic surfactants. *Environ. Sci. Technol.* **29**, 1480–1487 (1995).

49. Braida, W. J. *et al.* Sorption hysteresis of benzene in charcoal particles. *Environ. Sci. Technol.* **37**, 409–417 (2003).

50. Yang, Y., Shu, L., Wang, X., Xing, B. & Tao, S. Impact of de-ashing humic acid and humin on organic matter structural properties and sorption mechanisms of phenanthrene. *Environ. Sci. Technol.* **45**, 3996–4002 (2011).

51. Wen, B. *et al.* Phenanthrene sorption to soil humic acid and different humin fractions. *Environ. Sci. Technol.* **41**, 3165–3171 (2007).

Acknowledgments

Author contributions

K.S., J.J. and M.Q. designed the experiments, J.J. and Z.W. performed the sorption experiments, J.J., L.H. and Y.Y. conducted characterization, M.Q., B.G. and K.S. analyzed the data, M.Q., K.S., F.W. and B.X. co-wrote the paper. All authors reviewed the manuscript.

Additional information

Supplementary information accompanies this paper at http://www.nature.com/scientificreports

Competing financial interests: The authors declare no competing financial interests.

How to cite this article: Qiu, M.Y. *et al.* Properties of the plant- and manure-derived biochars and their sorption of dibutyl phthalate and phenanthrene. *Sci. Rep.* **4**, 5295; DOI:10.1038/srep05295 (2014).